

Experimental Studies on LMFBR Inner Vessel Models

R.Palaninathan¹⁾, G. Thomas¹⁾, M.R. Subash Chandra Bose²⁾, P. Chellapandi³⁾ and S.P. Damodaran³⁾

1) Department of Applied Mechanics, Indian Institute of Technology, Madras, India

2) Formerly Graduate Student, IIT, Madras; Presently Scientist, Naval Physical and Oceanographic Lab. Cochin, India

3) Indira Gandhi Centre for Atomic Research, Kalpakkam, India

ABSTRACT

This paper presents the results of an experimental study on the buckling of scale models of Liquid Metal Fast Breeder Reactor (LMFBR) inner vessel. The inner vessel consists of two cylindrical shells. The upper and the lower shells are connected by conical and torus shells. Six identical models are tested under three loading conditions. Imperfection scans are carried out using contact type probes, before loading and during loading. Scanning is carried out simultaneously for upper cylinder, conical, torus and lower cylinder using separate LVDTs and the data scanned is stored in a PC based data acquisition system. Strain gages are mounted at strategic locations and strains are recorded during load steps. Using the scanned raw data, initial geometric imperfections and eccentricity at different levels are calculated using a computer program. The results show that the imperfections grow with the load and the growth is predominant on lower cylinder and torus regions compared to that in conical and upper cylinder regions. The buckling loads are predicted analytically, using finite element method based, general purpose software, ABAQUS. The initial imperfections of experimental model are imposed on the analytical model in the form of eigen modes corresponding to the lowest buckling load with the amplitude equal to the highest imperfection measured. The experimental and analytical values are compared. In general, the experimental values are higher than the analytical values. Experiments have revealed scatter in the buckling values. Additional studies are required to arrive at some realistic conclusions.

INTRODUCTION

The two important structural components in the LMFBR are the main vessel and the inner vessel. These are characterised as 'thin shells', as the radius-to-thickness ratios are very high, ($R/t > 400$), higher than what is normally encountered in the aerospace structures. The shell structures are prone to fail by buckling, even at low stress levels. The exact estimation of buckling strength of prototypes /actual structures cannot be obtained through experimental programmes, because of the huge size. On the other hand, with the methods presently available to measure the geometric imperfections in actual structures and by incorporating the initial imperfections thus measured in the finite element modeling, it is possible to make use of the existing software packages for reasonably accurate estimation of buckling strength. However this approach needs to be validated through studies on scale models. The initial imperfections measured on the experimental models can be input in the finite element models of software packages. The analytical values thus arrived at can be compared with the experimental values. A correlation of the buckling strengths obtained by both means will lead to evolve a design procedure. This is the objective of the present study.

BRIEF HISTORICAL NOTES

The studies on shell buckling problems started about 150 years by Fairban in England and the motivation was the design of tubular bridges, a civil engineering application. The developments in boiler designs for mechanical and marine applications kindled further interest on shell buckling. Subsequently the advances in the aerospace field increased the awareness and the need for experimental studies on buckling of unstiffened and stiffened shells. Presently it is the nuclear industry attracting the attention of structural analysts to the buckling studies,[1,2]. The recent review papers by Teng [3] and Singer [4] present the historical developments. Most of the experimental studies were concerned with circular cylindrical shells, either under axial compression alone or external pressure alone or a combination of the two. Comparisons of experimental buckling stresses with the analytical predictions revealed wide difference between the two, particularly for the axial loading cases. The ratio of of experimental to predicted buckling loads, known as 'knock-down-factor' varied between 0.1 and 0.65 depending on the method of fabrication of the models. Also there were wide scatter between the experimental values. The reasons attributed for the discrebancy are [5]: effect of initial geometric imperfections, eccentricity in loading, influence of boundary conditions and prebuckling deformations. In view of the above reasons, the design of shell structures have to be relied more on experimental verifications. Large number of experimental studies carried out on scale models have been published in the open literature[6-8]. Mostly the models tested were made by machining or blow moulding or electro deposition etc. with desired imperfections; specified magnitude (as ratios of thickness-to-radius) and shapes (mostly

axisymmetric). Only very few studies have been carried on fabricated models [9]. The present work differs from the earlier studies in two respects: (i) the shape is of shell of composite geometry and (ii) the models possess the kind of initial geometric imperfections, similar to that possessed by the prototypes, which may be termed as 'real imperfections'.

BUCKLING EXPERIMENTS

Shell Models

The scale model (approximately 1/16th) of a typical LMFBR inner vessel is considered for the experiment. The test specimen consists of two cylindrical shells, a lower cylindrical shell of 420 mm nominal diameter and an upper cylindrical shell of 810 mm nominal diameter. The upper and lower cylinders are connected by conical and torus shells. There are six stand-pipes at the conical portion of the specimen. The sketch of the specimen used for the test is shown in Fig.1. Six identical shells are made from stainless steel (ASTM-304) sheets of 0.8 mm thick. The specimens are fabricated by three operations: rolling, welding and pressing in the case of torus and by the first two operations in the case of other parts.

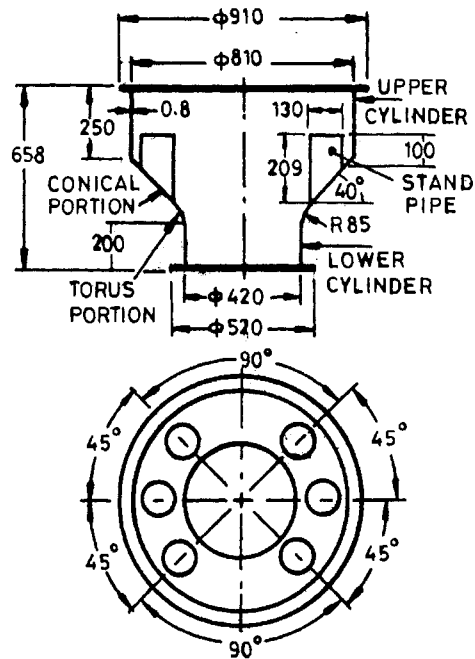


Fig.1 Test specimen geometric details

Loading Cases.

- Case -1: Concentrated load on the stand-pipe alone
- Case -2: Internal pressure alone
- Case -3: Combined stand-pipe load and internal pressure

Test Setup

The test setup consists of a loading frame, Hydraulic system for applying concentrated load on stand-pipes, air compressor for applying internal pressure, instrumentation and data acquisition system. The arrangement of the test setup is shown in Fig.2. The upper cylindrical portion of the specimen is connected to a bellow (4), which allows the free movement of the vessel during the loading. The bellow is connected to a top cover plate (3), which also carries the hydraulic jacks (5). The top cover plate is connected to the main loading frame (1) through an intermediate frame (2). The bottom cylindrical portion is connected to a cover plate (8), intermediate plate (9) and base plate (12). A freely rotating ring (11) is located around the intermediate plate for mounting the linear voltage differential transformers(LVDTs). The total vessel assembly is supported at the bottom through three load cells placed at 120 degrees apart (13). Strain gages are bonded on the torus and lower cylindrical areas where maximum deformations and buckling are expected to occur. There are: four LVDTs for the measurement of imperfections around the vessel at conical, torus, lower and upper cylindrical portions. The LVDTs and strain gages are connected to a

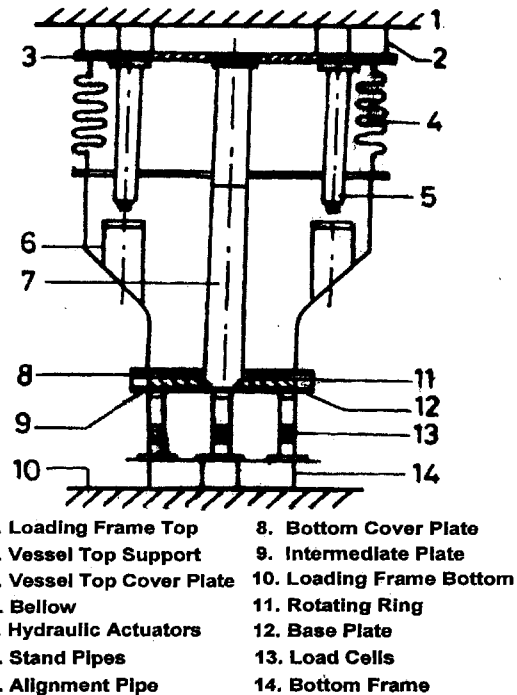


Fig.2 Details of experimental setup

personal computer based data acquisition system (Micro measurements, USA). The three load cells and the pressure transducers are connected to the 6-channel carrier frequency amplifier (HBM make).

Loading System

The actuators are loaded by a hydraulic system consisting of a motor and pump and moved until all the six actuators make contact onto the stand-pipes. The actual loading of the specimen by actuators are assisted by a pneumatic system called intensifier, which helps to apply a smooth and gradual loading. The pneumatic loading is effected by the gradual loading of the intensifier through an air pressure regulator. The air pressure inside the vessel is applied from a compressor through a regulator allowing gradual loading.

Instrumentation

- a) **LVDT**: Four LVDTs are used for measurement of imperfections at the lower cylinder, torus, conical and upper cylinder. Make : HBM / Syscon. Range :- ± 10 mm FS sensitivity : 80mV/V/mm for HBM and 600mV/V/mm for Syscon.
- b) **Pressure Transducers** : Specially designed transducers are used for the measurement of air pressure in the vessel chamber and oil pressure in the hydraulic system for precise and gradual loading of the specimen. Make : Developed in house. Range : 0-2.5 kg/ cm² for vessel chamber air pressure. 0-250 kg/ cm² for the hydraulic system.
- c) **Pressure Gauges**: Bourdon type pressure gauges are used to monitor the air pressure supply to the hydraulic intensifier, vessel chamber and oil pressure in the hydraulic system. Make : Local; Range : 0-10 kg/ cm² for air pressures and 0-250 kg/ cm² for oil pressure.
- d) **Pressure Regulator**: The precise control of air flow to the hydraulic intensifier and vessel chamber is achieved using air regulators. They can control the flow of air upto 0.001 kg/ cm² very accurately. Make : Festo controls, Range: 0-4 kg/ cm²
- e) **Load Cells**: The loading on to the vessel is measured using custom made load cells designed and manufactured in house. They are designed as an integral part of the three-point bottom support of the vessel. Range: 0 - 5000 kg.
- f) **Strain Gages**: Strain gages are fixed at the torus, upper and lower cylindrical areas. Make:- Measurement Group , USA. Range: $\pm 5\%$ of gage length.
- g) **Data Acquisition System**. : The system has a 16- bit A/D converter and scanning rate of 1 ms per scan. The strain gages and the LVDTs are connected to a computer controlled data acquisition system.
- h) **Carrier Frequency Amplifier**: The three load cells and the pressure transducers are connected to the 6-channel carrier frequency amplifier (HBM make).

Imperfection Measurement System:

The imperfection measurement system consists of a wheel, an outer ring, a base plate and an indexing mechanism as shown in Fig. 3. The outer ring is capable of rotation over the rim of the load bearing wheel. The outer ring is also supported at the bottom by six caged steel balls. On the outer ring, arrangements are made for rotation at fixed intervals, ie 10 degrees. The indexing mechanism consists of a spring loaded plunger which can slip into 36 holes made on the periphery of the bottom supporting plate at 10 degree intervals. Brackets are provided with pillars on the outer ring for mounting the LVDT. The position of the LVDTs can be adjusted to different axial locations at specific height intervals . The LVDT for the torus and conical portions are provided with rotational arrangement in the vertical plane to fix at specific angles and are mounted on separate brackets. The center of rotation of torus LVDT coincides with the center of curvature of the torus and hence it can be mounted at any angle normal to the surface the torus (the torus radius is 85 mm). The LVDT for cone is mounted at a particular angle, normal to the surface, 50 degree from horizontal. The imperfection measurements are taken around the circumference at equally spaced intervals. It is necessary to fix the axis of the measuring system (LVDT axis) as close as possible to that of the specimen. The radial measurements are to be corrected for the mean and for the error in positioning the system. The initial imperfections, δ_i are deduced from the following equation:

$$\delta_i = \Delta r_i + \Delta r' - a \sin \theta_i - b \cos \theta_i$$

where Δr_i - LVDT reading at station i

$$\Delta r_i = -\frac{\sum \Delta r_i}{n}, \quad a = \frac{2}{n} \sum \Delta r_i \sin \theta_i, \quad b = \frac{2}{n} \sum \Delta r_i \cos \theta_i$$

θ_i - angular position of station i

$$\text{Eccentricity, } e = (a^2 + b^2)^{1/2}$$

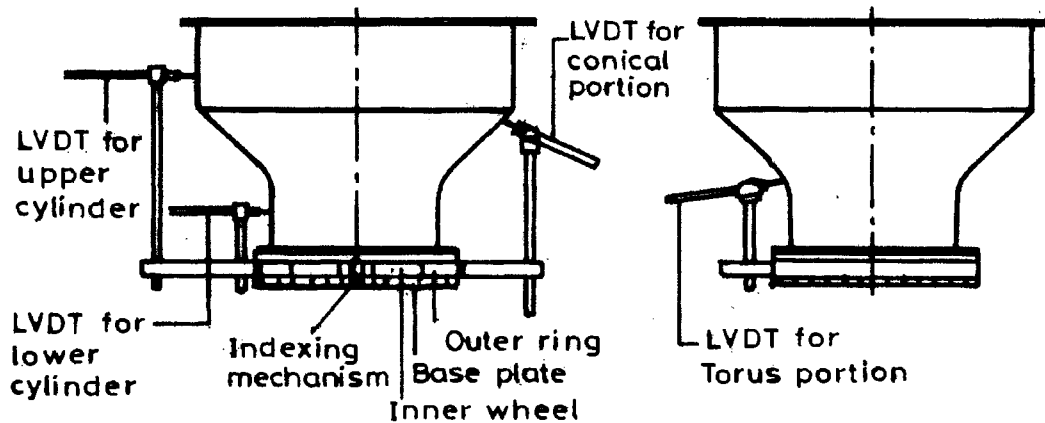


Fig.3 Imperfection measurement system

Test Procedure

Imperfection Measurement

Firstly the initial geometric imperfection measurements are carried out simultaneously at all four regions; torus, conical, lower and upper cylindrical areas and the data is stored in the computer using a data acquisition system. After one sweep, the LVDTs are shifted/rotated for next level. On the lower cylinder, measurements are taken at four levels; 40, 80, 120 and 160 mm height from the lower flange. On the upper cylinder, measurements are taken at 215, 175, 135 and 95 mm from the upper flange. On conical area readings are taken at 35mm, 25mm, 15mm and 5mm from upper cylinder-cone junction. Similarly, on torus area, readings are taken at 0, 10, 15 and 20 degrees to the horizontal. The scans are carried out at some load steps also to plot the deformation pattern with load.

Loading

The hydraulic system is operated to bring the actuators onto the stand-pipes and then with the pneumatic assistance, using the intensifier, axial load is applied to the specimen. The hydraulic loading is applied to the pre-determined level by adjusting the intensifier pressure. Then air pressure is applied in the shell chamber by controlling the air regulator for the combined loading case. For internal air pressure loading case no hydraulic load is applied and for axial load case no air pressure is applied in the shell chamber. During the loading, at some steps, the LVDT scans are taken. The strain gage, load cell and pressure transducer readings are also recorded. The loading is continued until the specimen fails. The LVDTs are removed when the loading is about 75% of the predicted failure load to prevent the damage of LVDTs. The onset of buckling is visually observed from the formation of buckling lobes.

TEST RESULTS

Internal Pressure Load

The experiments on shell #2 and #4 are conducted with internal air pressure alone. The initial geometric imperfections and eccentricity, e between specimen and LVDT axes are calculated using the computer program developed. The eccentricities, e are found to be 1.64 mm for shell #2 and 3.14 mm for shell #4 on upper cylinder. The geometric imperfections for shell #2 in the torus are shown in Fig.4. The deformation patterns are also measured during the loading. The deformed configurations in the torus are shown in Fig. 5. The maximum initial imperfection on lower cylinder is 1.46 mm which increases to 2.04 mm with 730 mbar pressure. Similarly on torus area the maximum initial imperfection is 1.2 mm which increases to 1.80 mm. The buckling lobes are formed first which is followed by collapse with a "thud" sound. The shell #2 buckles at a pressure of 0.9 bar and shell #4 buckles at 0.96 bar against the predicted pressure of 0.95 bar by ABAQUS. The experimental value is 95% of ABAQUS results for shell #2 and 101% for shell #4. The finite element modeling incorporated the initial

imperfections obtained from the experiment. The method may be termed as “eigen mode injection”, which is a conventional one. In this method, the mode shape corresponding to the lowest buckling load of the perfect shell is obtained. The amplitude of the wave form is set equal to the maximum imperfection measured in the experiment. Subsequently, the nonlinear analysis is carried out using the “imperfect FE model”. The limit point value is taken as the buckling load. If the finite element modeling does not incorporate the initial imperfections, the analytical value would have been much higher. It is to be noted that the actual imperfections present in the experimental models have not been incorporated in FE models.

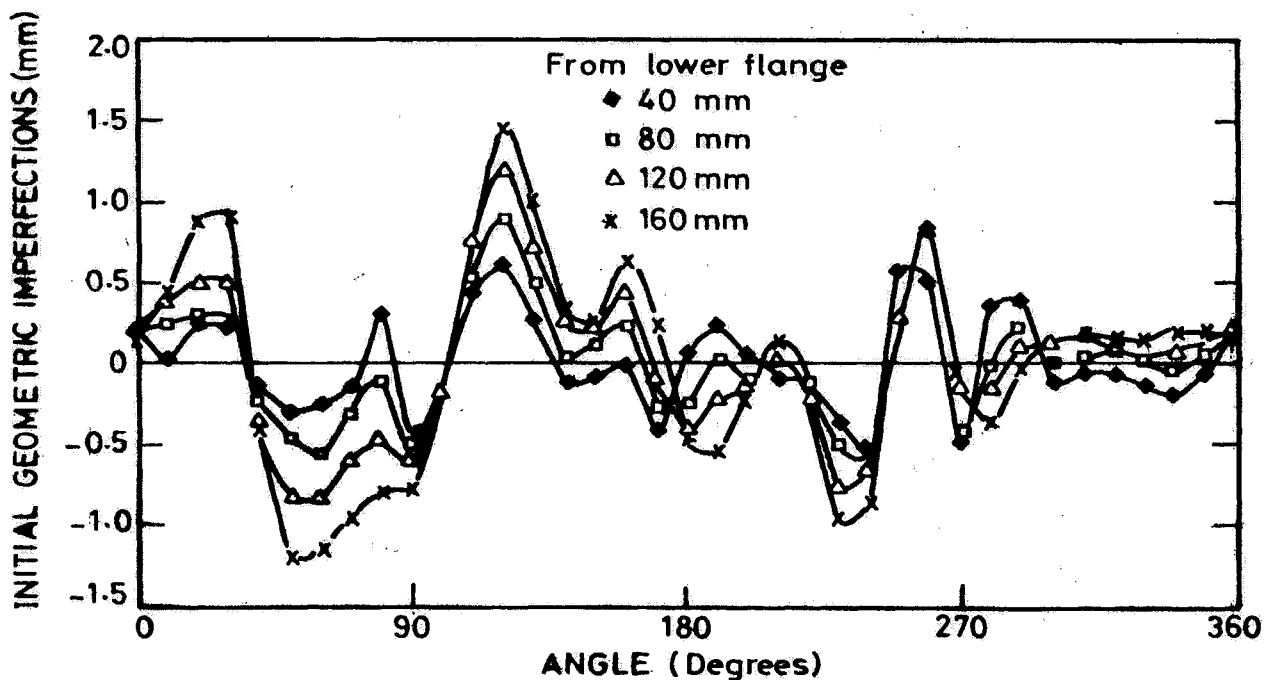


Fig.4 Initial geometric imperfections in lower cylinder, shell # 2

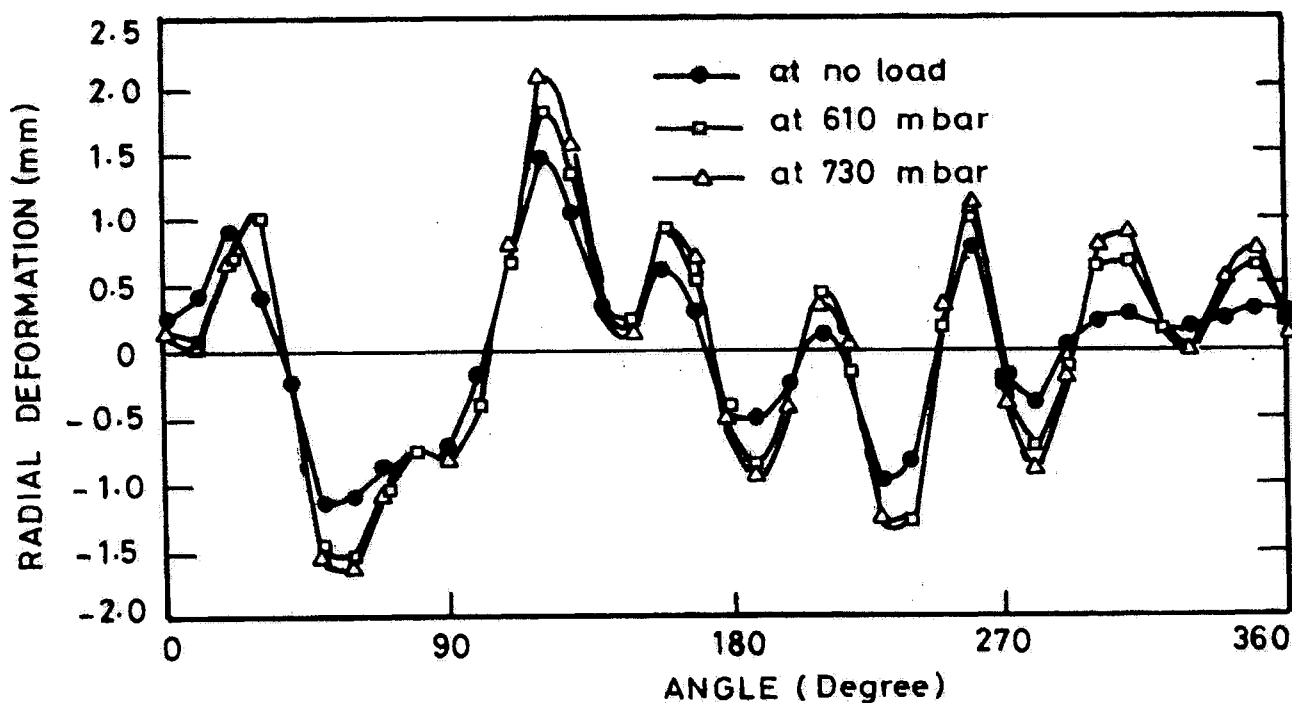


Fig.5 Radial deformation with internal pressure in lower cylinder, shell #2

Concentrated Load on the Stand-pipes

The experiments on shell #3 and #5 are conducted with axial load alone. Initial imperfections are measured at lower cylinder, torus, cone, and upper cylinder areas at various locations as in the previous case. The maximum eccentricity is found to be 1.09 mm on torus region for shell #5 and 8.03 mm for shell #3 on upper cylinder. The high eccentricity was due to the manufacturing deviations. The geometric imperfections at various locations are plotted. The deformations are also measured during loading. The deformation patterns, which resembles more or less that of the initial imperfections, grow with axial load and are substantial on lower cylindrical and torus regions. On lower cylinder region (160 mm from lower flange) the maximum geometric imperfection at no-load is found to be -0.97 mm and the same increases to -1.35 mm with a load of 14274 N. Similarly on torus region (0 degree to horizontal) the maximum geometric imperfection at no-load is 1.04 mm and it increases to 1.65mm with a load of 14274 N. The growth is minimal at the conical and upper cylindrical areas. It is also observed that the growth of imperfections with axial load is more compared to the pressure load alone case. The strains at different locations are recorded for various loads. The shell #3 buckles at a load of 16137 N and shell #5 buckles at 18149 N against the predicted value of 13989 N by ABAQUS. The onset of buckling is noticed by visual observation of lobe formation. The lobes are formed in the torus region below the stand-pipes. The model is coated with a light coat of non-reflecting paint and grid lines are marked for better visualisation of buckled shape. However, it is found that the painting of the surface does not improve the visualisation and hence it is not used for other models. The experimental value is more than 15% of ABAQUS results for shell #3 and 30% for shell #5.

Combined Load

The shell #1 and shell #6 are tested under combined load case, wherein the stand-pipe load is applied in 6 steps to 11772N and subsequently the pressure is applied in steps of 25 millibar upto 100 millibar and then in steps of 10 millibar till the failure takes place. The geometric imperfections along the circumference for various locations are plotted. The deformation patterns with load is maximum on lower cylinder and torus area. The growth is negligible on conical and upper cylindrical area. The shell #1 fails at 11772 N (1200 kg) axial load and 0.118 bar internal pressure against the predicted value of 11772 N (1200 kg) and 0.151 bar by ABAQUS. The experimental value is about 16% more than the predicted value. The onset of buckling is noticed by visual observation of lobe formation. In the case of Shell #6, the failure occurs at axial load of 11772 N and air pressure of 0.305 bar, which works out to a total load of about 23544 n (2400 kgf). The failure occurs in the torus region, exactly below the stand-pipes. The analytical model predicts the same failure mode. Twelve strain gages are used for the measurement of strains at different locations around the torus region as shown in Fig. 6. The strain gages are bounded at the inner and the outer surfaces at a location. A special fixture is used to mark the locations exactly. The variations of strains with load of all 12 gages are recorded, out of which the responses of 4 gages (Nos. 1, 6,7 and 12) are shown in Figs 7 and 8. As seen from these figures, initially membrane state of strain/stress exists, as indicated by more or less equal values of strains between the two gauges in a pair. As the buckling load is reached, there are sudden changes in the values of strain gage pairs, going in the opposite directions. This indicates the change of state from membrane to bending conditions. This helps to pin-point the buckling load graphically.

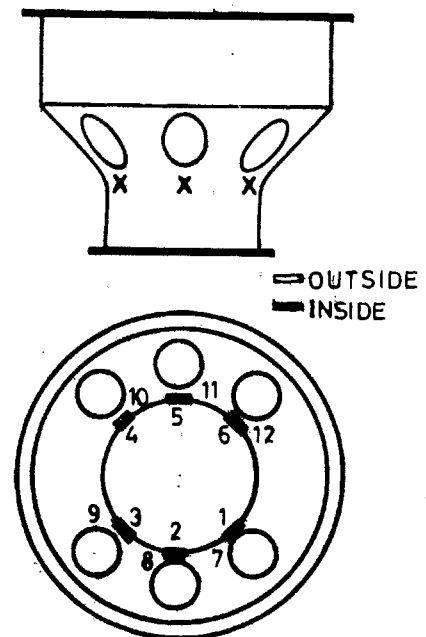


Fig.6 Strain gage locations, shell #6

SUMMARY

The overall results of the six experiments are summarised in Table 1. It may be noted that the experimental values are in general larger than the analytical ones. The reason for the analytical values being lower than the experimental values may be explained from the fact that the 'eigen mode injection method' has been employed in finite element modeling. The eigen mode for the shell models, as determined by ABAQUS has several half waves in the circumferential direction ($n = 10$). Hence the imperfection imposed on the FE model is considerably high. In one case (Model # 5 under axial load), the

difference is 30% and in another case (Model # 6 under combined load), the difference is 100%. With the available data, it is difficult to explain this large difference. The 1/16th scale models, fabricated using conventional methods are found have initial imperfections in the range of -3.5 to 6 times the thickness. However, the imperfections in the critical region, namely, the torus, in the present case, is important. By and large the deformation with load follows that of the initial imperfection shape. The failure starts below stand-pipes in the torus region in all cases.

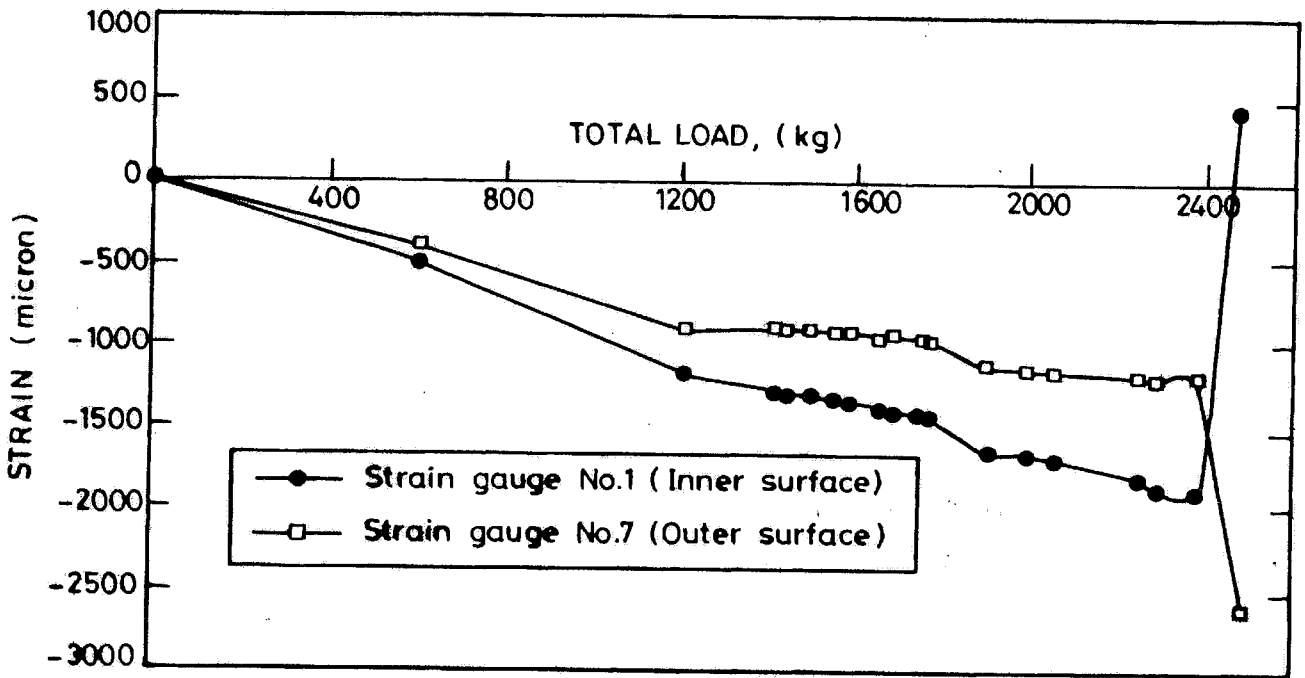


Fig.7 Variation of strain with load in torus region, shell # 6 (Gauge Nos.1 and 7)

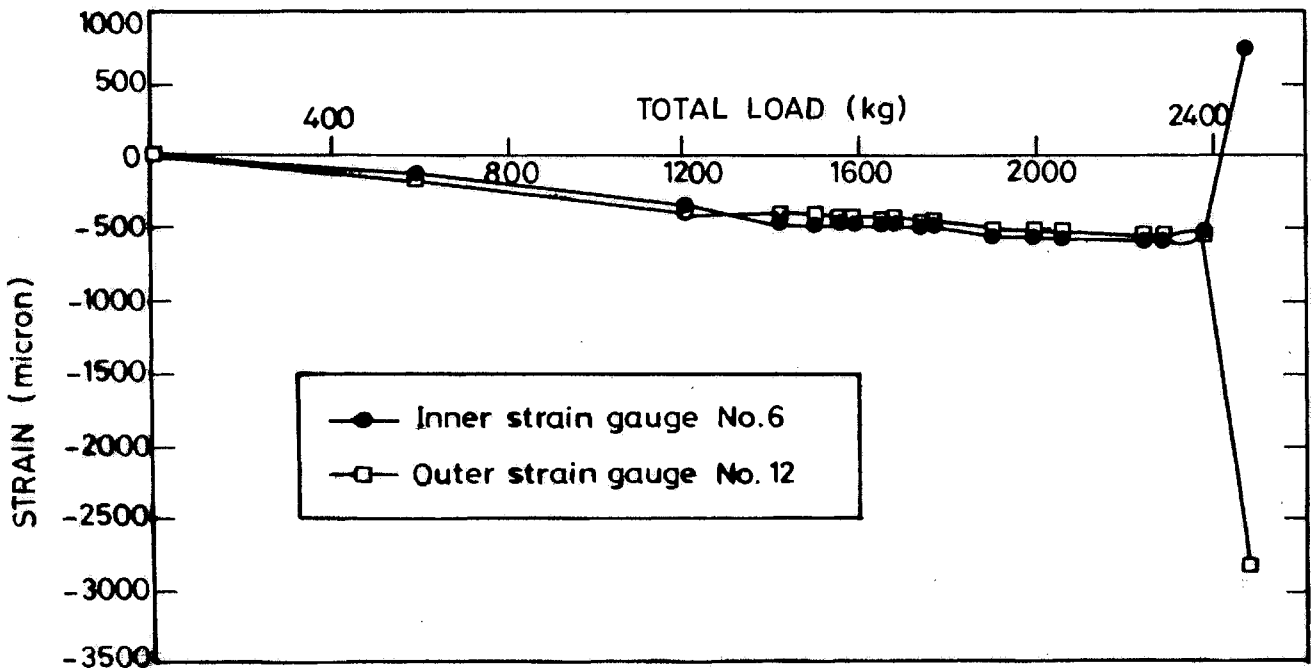


Fig.8 Variation of strain with load in torus region, shell # 6 (Gauge Nos.6 and 12)

Table1. Initial Imperfection, Eccentricity, Experimental and Analytical Buckling Loads

Shell No.	Loading Details	Max. INITIAL GEOMETRIC IMPERFECTION (mm)				BUCKLING LOAD				P_{EXP}/P_{PR}
		Lower cylinder	Torus	Cone	Upper cylinder	Experiment (P_{EXP})		Predicted (P_{PR})		
						Stand pipe load N (kg)	Pressure (bar)	Stand pipe load N (kg)	Pressure (bar)	
1	Combined axial and pressure	-1.12 to 1.10	-1.68 to 1.34	-1.14 to 1.3	-1.81 to 0.90	11772 (1200)	0.175	11772 (1200)	0.151	1.16
2	Pressure alone	-1.2 to 1.44	-1.36 to 1.36	-2.27 to 1.52	-1.30 to 1.69	0	0.90	0	0.95	0.95
3	Axial load alone	-2.52 to 1.23	-1.19 to 1.1	-2.86 to 1.67	-1.76 to 2.5	16137 (1645)	0	13989 (1426)	0	1.15
4	Pressure alone	-0.72 to 0.73	-0.75 to 1.00	-2.32 to 2.03	-2.08 to 3.04	0	0.96	0	0.95	1.01
5	Axial load alone	-1.53 to 1.22	-0.85 to 1.64	-1.52 to 1.71	-3.13 to 4.36	18149 (1850)	0	13989 (1426)	0	1.30
6	Combine d axial and pressure	-2.33 to 1.3	-1.89 to 2.41	-1.86 to 3.82	-3.57 to 3.46	11772	30500	11772	15100	2.02

REFERENCES

1. Combesure,A., "Static and Dynamic Buckling of Large Thin Shells", Nuclear Engineering and Design, Vol. 92, 1986, pp. 339-354
2. Matsuura,S., H.Nakamura, S. Ogiso, Y.Ooka and H. Akiyama, "Buckling Strength Evaluation of FBR Main Vessel under Lateral Seismic Loads", SmiRT 11 Transactions, Vol. E,Tokyo, Japan, August, 1991, pp. 269-280.
3. Teng,J.G., "Buckling of Thin Shells: Recent Advances and Trends", ASME, Applied Mechanics Review, Vol. 49, 1996, pp. 263-274.
4. Singer, J., "Experimental Studies in Thin Shell Buckling", Proc. Structural Dynamics and Materials Conf., American Institute of Aeronautics and Astronautics, New York, Vol.3, 1997, pp.1922-1932
5. Arbocz, J. and Babcock, Jr. C.D., "The Effect of General Imperfections on the Buckling of Cylindrical Shells", ASME, J. of Applied Mechanics, March, 1969, pp.28-38.
6. Anon., "Collected Papers on Instability of Shell Structures-1962", NASA TN D-1510, Langley Research Center, Langley Station, Hampton, Va., USA.
7. Schneider, Jr. M.H., "Investigations of the Stability of Imperfect Cylinders using Structural Models", Engineering Structures, Vol. 18, No.10, 1996, pp.792-800.
8. Wackel, N., J.F.Jullian and P.Ledermann, "Experimental Studies on the Instability of Cylindrical Shells with Initial Geometric Imperfections", ASME, J. of Pressure Vessel and Piping, Vol. 89, 1984, pp. 33-42.
9. Knoedel, P., Thomas Ummenherfer and Ulrich Schulz, "On the Modeling of Different Types of Imperfections in Silo Shells", Thin-Walled Structures, Vol.23, 1995, pp.283-293.

ACKNOWLEDGEMENT

The Investigators express their sincere thanks to the authorities of Indira Gandhi Centre for Atomic Research, Kalpakkam, for having sponsored this project. Particularly we thank Mr.S.B.Bhoje, Director and Mr.S.C.Chetal, Associate Director, Design and Technology Group for their keen interest and active participation during the execution of the project. Also, the authors express their sincere thanks to Mr.A.Sadasivam, Supervisor, Department of Applied Mechanics, Indian Institute of Technology, Madras for valuable assistance in the fabrication of experimental setup and in conducting the experiments.